Weak ferromagnetism and spin-charge coupling in single-crystal Sr_2YRuO_6

G. Cao, Y. Xin, C. S. Alexander, and J. E. Crow

National High Magnetic Field Laboratory, Tallahassee, Florida 32310

Sr_2YRuO_6 is a magnetic insulator with a double-perovskite structure derived from the perovskite $SrRuO_3$, which is an itinerant ferromagnet. Measurements of the magnetic susceptibility, magnetization, and electrical resistivity are performed on newly synthesized single crystals of Sr_2YRuO_6. The system orders antiferromagnetically at $T_N = 26$ K and yet shows a conspicuous occurrence of weak ferromagnetism characterized by large irreversibility in both magnetic susceptibility and isothermal magnetization. The ordered magnetic moment at 7 T shows weak temperature dependence and is only $0.5\mu_B/Ru$, substantially low compared to that expected for an $S = 3/2$ system, consistent with weak ferromagnetism. The electrical resistivity demonstrates a weak temperature dependence from 800 to 160 K and a rapid rise in the lower-temperature range. A sharp anomaly in the resistivity is observed at the magnetic ordering temperature T_N, which is then followed by a Mott-like transition at $T_M = 17$ K. The system also exhibits sizable negative magnetoresistance, which persists well above the magnetic ordering temperature. All results presented reveal unusual magnetic and transport properties that underscore the strong interplay of spin, charge, and orbital degrees of freedom.

Studies of layered ruthenates or Ruddlesden-Poper series $(Ca, Sr)_{n+1}Ru_nO_{8n+1}$ in the last few years[1–14] have revealed a richness of intriguing and complex physical phenomena. These materials, often characterized by a strong competition between antiferromagnetic and ferromagnetic coupling and a complex interplay of spin, charge, and orbital degrees of freedom, are extremely sensitive to small perturbations such as slight structural alterations. As an extension of our work on the layered ruthenates, we have recently investigated the double perovskite Sr_2YRuO_6 in *single-crystal* form, which was noticeably not available before. Sr_2YRuO_6 is known to be an antiferromagnetic insulator.[15,16] The Ru ion in this compound is pentavalent $(4d^3)$ and in a high-spin state $(^4A_{2g})$ with $S = 3/2$ instead of tetravalent $(4d^4)$ and a low-spin state $(^3T_{1g})$ with $S = 1$ as in the members of the Ruddlesden-Poper series of the ruthenates. Sr_2YRuO_6 adopts a crystal structure derived from the itinerant ferromagnetic perovskite $SrRuO_3$ by replacing every another Ru by Y so that the remaining Ru ions form an fcc lattice. In spite of the apparent phase proximity to itinerant ferromagnetism and, to some extent, superconductivity observed in Sr_2RuO_4, the ground state of Sr_2YRuO_6 is vastly different from those of its sister compounds and thus underlines the subtlety of the magnetic and electronic structure, which very often typifies perovskitelike ruthenates.

Although Sr_2YRuO_6 was first synthesized more than 20 years ago,[15–17] only recently have there been a handful of reported experimental and theoretical[18] studies driven partially by an attempt to search for superconductivity and its coexistence with ferromagnetism, which were reportedly found in Sr_2YRuO_6 with dilute Cu doping.[19–21] While superconductivity is beyond the scope of this paper, it is our intention to gain insight into the nature of the ruthenates in general and systematically characterize the magnetic and transport properties of Sr_2YRuO_6 in particular. Investigations of this system were previously carried out only on *polycrystalline* samples primarily using powder neutron diffraction and measurements of magnetic susceptibility below 70 K.[17]

Based on these earlier studies, the system possesses two major features: namely, it is antiferromagnetically ordered at 26 K with a type-I spin configuration and an ordered magnetic moment of $1.85\mu_B/Ru$ (Ref. 17) and it is insulating although no results of electrical resistivity have ever been reported.

In this paper, we report the results of magnetic and transport studies obtained from Sr_2YRuO_6 single crystals, which are particularly crucial for oxides containing Sr and Ru due to the frequently unavoidable presence of precursor phases such as strongly ferromagnetic $SrRuO_3$ $(T_C = 165$ K) in polycrystalline samples (only a few percent of the $SrRuO_3$ phase often overshadows or distorts intrinsic magnetic properties of underlying materials). While our data show a magnetic ordering at $T_N = 26$ K consistent with that reported for the polycrystalline samples, many unusual features that are conspicuously absent in polycrystalline Sr_2YRuO_6 have been observed. In particular, the magnetic susceptibility below T_N becomes highly hysteretic, suggesting the occurrence of weak ferromagnetism, not uncommon in $4d$ and $5d$ oxides due to the strong spin-orbit coupling. Weak ferromagnetism is also evidenced in the isothermal magnetization that is irreversible and nonlinear though far from being saturated. The magnetic moment extracted at $H = 7$ T is weakly temperature dependent below 40 K and surprisingly low compared to that expected for an $S = 3/2$ system. Sr_2YRuO_6 displays nontrivial conducting behavior obeying no obvious power law or exponential throughout most of the temperature range measured $(1.5 < T < 800$ K). Furthermore, a well-defined anomaly in resistivity is observed at the Néel temperature T_N, which is then followed by a Mott-like transition at $T_M = 17$ K. All results seem to point out spin-charge coupling and a competition between antiferromagnetic and ferromagnetic coupling, which is in accordance with results of band structure calculations for Sr_2YRuO_6.[18]

Single crystals were grown in Pt crucibles using the flux technique from off-stoichiometric quantities of RuO_2, Y_2O_3, $SrCO_3$, and $SrCl_2$. The mixed chemicals were heated at 1500 °C for 20 h and slowly cooled down at a rate of 2 °C/h
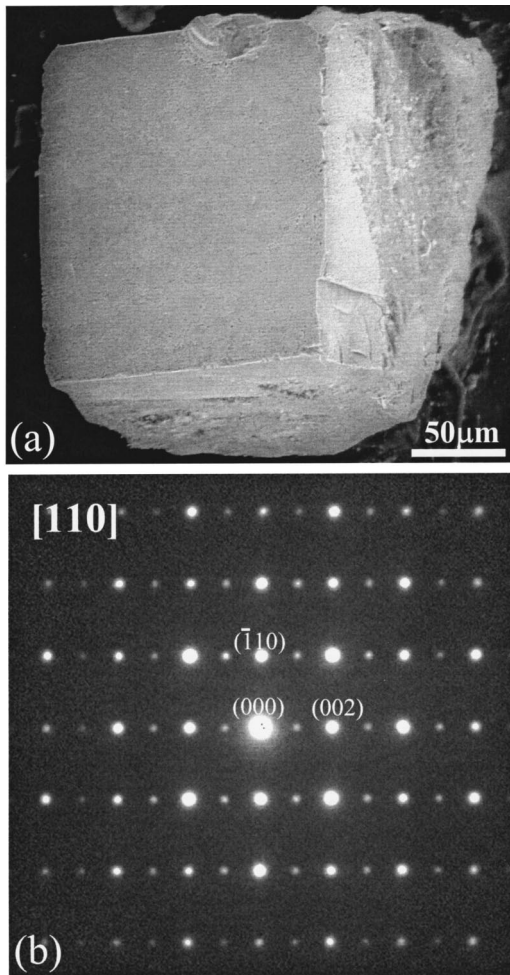
FIG. 1. (a) SEM image of a single Sr_2YRuO_6 crystal; (b) TEM diffraction pattern of [110] from the crystal.

to 1350 °C and finally quenched to room temperature. The single crystals were fully characterized by electron microscopy and x-ray diffraction. Resistivity was measured with a standard four-probe technique and magnetization with a commercial superconducting quantum interference device magnetometer.

The resulting shape of Sr_2YRuO_6 single crystals tends to be cubiclike with an average size being $0.15 \times 0.15 \times 0.10$ mm^3. The typical morphology of the single crystal is shown in Fig. 1(a), which is a secondary electron image from a scanning electron microscope (SEM). It is clear that the crystal is formed with flat and low-indexed planes. The lump attached to the sides of the crystal is the remains of the flux. The individual Sr_2YRuO_6 single crystals were also characterized by transmission electron microscopy (TEM) using a JEOL 2010 microscope operated at 200 kV. The composition of the crystal is examined by energy-dispersive x-ray spectroscopy (EDS), confirming the ratio of Sr:Y:Ru being 2:1:1. Figure 1(b) displays a selected-area diffraction pattern of the [110] zone axis obtained from a thin area of about 170 nm thick determined by two-beam convergent beam electron diffraction from such a crystal as shown in Fig. 1(a), whose sharp reflections are characteristic of a single crystal. The simulation of the diffraction pattern using the crystal struc-
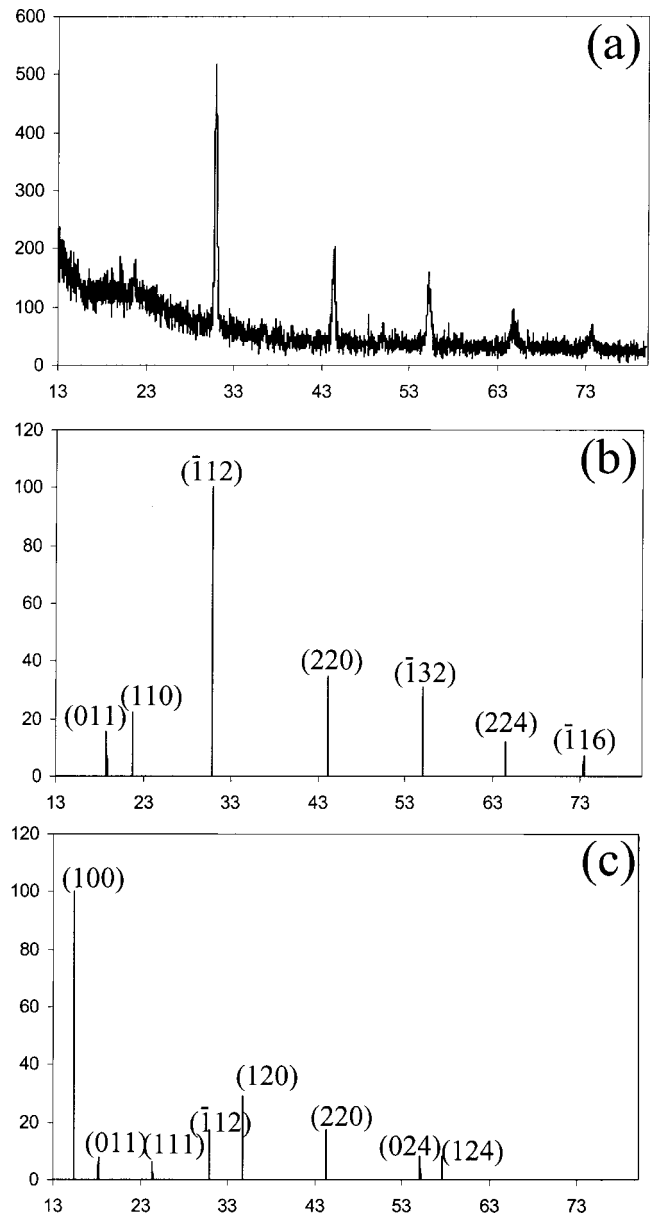
FIG. 2. (a) Experimental x-ray diffraction pattern from powered single crystals; (b) calculated diffraction peaks using the perfect Sr_2YRuO_6 structure; (c) calculation using models with disordering of Y and Ru or long-range order vacancies.

ture reported[17] is consistent with the experimental data.

X-ray diffraction from powdered single crystals was carried out using a Scintag powder diffractometer, as shown in Fig. 2(a). The crystal structure of the single crystals is confirmed to be the same as one reported in Ref. 17. To ensure that these single crystals have the ordered stacking of Ru-O and Y-O octahedra in this double perovskite, as previously reported,[17] calculations using several structural models were performed to estimate the relative intensities of the *major* diffraction peaks using DesktopMicroscopist software [Figs. 2(b) and 2(c)]. The ordering of Ru and Y in Sr_2YRuO_6 is verified by results of the calculations where the relative intensities are in a perfect agreement with the experimental data with the (-112) peak being the strongest [Figs. 2(a) and
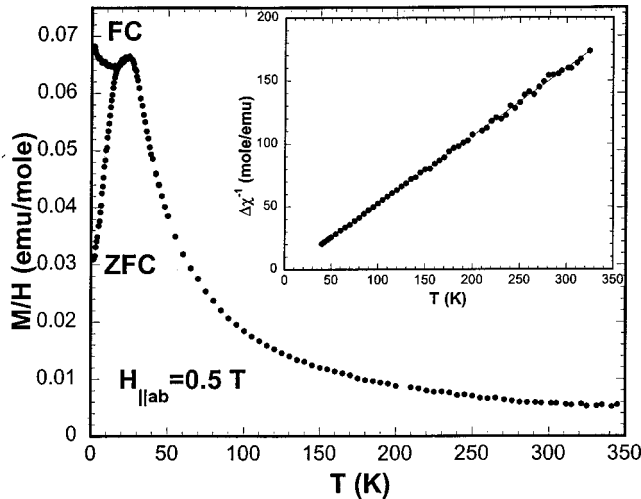
FIG. 3. Zero-field-cooled (ZFC) and field-cooled (FC) magnetic susceptibility (defined as M/H) as a function of temperature at $H_{\|ab}=0.5$ T. Inset: reciprocal magnetic susceptibility as a function of temperature.

2(b)]. In sharp contrast, should there exist a disordered stacking of Ru and Y ions or long-range order vacancies in the structure, the (100) peak would become the strongest one instead with a largely diminished (-112) peak [Fig. 1(c)]. In fact, assuming disorders or vacancies even as small as 1% at Ru and Y sites in the calculations could result in drastic changes in the relative intensities. The results displayed here unambiguously prove that single-crystal Sr_2YRuO_6 possesses ordered crystal structure without any disordering or long-range order vacancies, consistent with results reported previously.[17]

The crystal structure of Sr_2YRuO_6 is a derivative of the perovskite $SrRuO_3$ by replacing every another Ru by Y. It becomes monoclinic due to the larger ionic radius of Y with a space group of $P2_1/n(14)$ and unit cell parameters $a=5.7690$, $b=5.7777$, $c=8.1592$ Å, and $b=90.23°$.[17] Ru-O and Y-O octahedra are all tilted away from their ideal cubic orientation with long Y-O bond length (2.2 Å) and a short Ru-O bond length (1.95 Å).[17] Unlike in $SrRuO_3$, there are no common O ions shared by neighboring Ru-O octahedra in Sr_2YRuO_6; each Ru-O octahedra shares a single O atom with each neighboring Y-O octahedra. The π superexchange between the nearest Ru ions is carried out via a Ru-O-O-Ru linkage and the σ superexchange via a Ru-O-Y-O-Ru linkage. However, the Y ions are not expected to play a significant role in the magnetic superexchange because they are fully ionized and provide no accessible orbitals necessary to participate in superexchange. Sr_2RuYO_6 can be thus considered as consisting of tilted RuO_6 octahedra which are connected via two bridging O atoms.

Shown in Fig. 3 is the temperature dependence of the magnetic susceptibility defined as M/H for the ab plane in a field-cooled (FC) and zero-field-cooled (ZFC) sequence with magnetic field $H=0.5$ T. While evidence for the magnetic phase transition is obvious at $T_N=26$ K, the magnetic susceptibility becomes highly hysteretic. This behavior, unexpected for an ordinary antiferromagnet, indicates the occurrence of weak ferromagnetism, which will be discussed below.

Fitting to a modified Curie-Weiss law for $40<T<350$ K yields an effective paramagnetic moment of $\mu_{eff}=3.87\mu_B/$Ru that is in perfect agreement with the theoretical value for $Ru^{5+}(4d^3)$ ions determined by the spin-only formula $\mu_{eff}=2[S(S+1)]^{1/2}\mu_B$ (see the inset of Fig. 3). This result, however, differs from that reported in an earlier study where μ_{eff} was found to be $3.13\mu_B/$Ru, which was attributed a spin-orbit coupling.[16] The Curie-Weiss temperature $\Theta_{CW}=-2.5$ K, one order of magnitude smaller than T_N, suggests a weak antiferromagnetic exchange interaction or the coexistence of comparable ferromagnetic interactions. Nevertheless, this result is considerably different from one reported earlier where $\Theta/T_N=5.5$ for polycrystalline Sr_2YRuO_6.[16] The temperature-independent magnetic susceptibility χ_O is estimated to be 1.1×10^{-3} emu/mol, which is large for insulators. The enhancement in χ_O, known as the Stoner enhancement and commonly seen in oxides with a narrow band, may imply a magnetic instability driven by spin fluctuations or a strong competition between antiferromagnetic and ferromagnetic coupling that is also manifested in band structure calculations.[18]

The existence of weak ferromagnetism becomes unambiguous in Fig. 4, which displays the temperature dependence of the ZFC and FC magnetic susceptibility for different magnetic fields ($H=0.02$, 0.5, and 4 T) below 60 K. At $H=0.02$ T, the magnetic susceptibility shows a sharp transition strikingly similar to that of a spin glass. As the magnetic field H increases, the transition becomes largely broadened, whereas the magnetic irreversibility decreases and yet remains to be significantly large. At $H=4$ T, the magnetic susceptibility resembles a ferromagnet rather than an antiferromagnet. In fact, the broadening of the magnetic transition with increasing H is a characteristic of a ferromagnet. In contrast, for an ordinary antiferromagnet increasing magnetic field only suppresses the Néel temperature, but retains the sharpness of the transition. It is also expected for an antiferromagnet to show a different temperature dependence of the magnetic susceptibility for different principal crystallographic directions below the Néel temperature. The magnetic susceptibility of Sr_2YRuO_6 shows no significant anisotropy below $T_N=26$ K when measured with H parallel to the a and c axes [see Fig. 4(a)]. While it cannot be ruled out that this behavior could be due to yet undetected microscopic disorder inherent to this material, which would in turn lead to glassy behavior, it is much more likely that there is a strong competition between antiferromagnetic and ferromagnetic coupling, which leads to canted antiferromagnetism or weak ferromagnetism. There are two possibilities for the occurrence of weak ferromagnetism in the absence of itinerant electrons, namely, single-ion magnetic anisotropy and antisymmetric superexchange. It is plausible that the noncubic crystal field and spin-orbit coupling, which is always significant in $4d$- and $5d$- electron oxides where d orbitals are extended, create local anisotropy energies which in turn cant spins to induce a small, ferromagnetic component when minimized.[22] However, the presence of weak ferromagnetism could also be attributed to an antisymmetric exchange
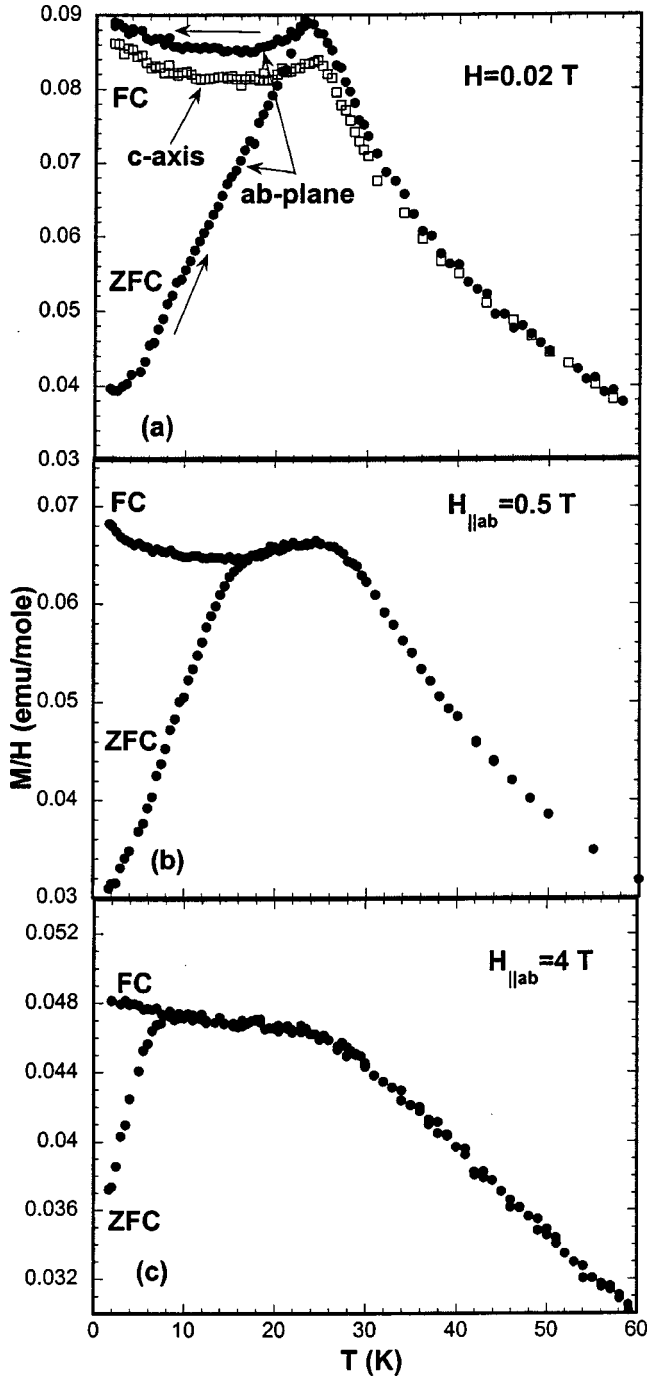
FIG. 4. Zero-field-cooled (ZFC) and field-cooled (FC) magnetic susceptibility as a function of temperature at $H_{\|ab}=0.02$ T, (a), 0.5 T (b), and 4 T (c). Field-cooled magnetic susceptibility for the c axis is also plotted in (a).

interaction or Dzyaloshinskii-Moriya interaction[23,24] motivated by a lack of inversion symmetry of the Ru atoms.

Shown in Fig. 5 is the isothermal magnetization M for the ab plane. There are a few features that are remarkable. (1) M is hysteretic, characteristic of a ferromagnet [see Fig. 5(a)]. The irreversibility becomes smaller and eventually vanishes as T increases. The remnant ferromagnetic moment extrapolated to $H=0$ is about $0.05\mu_B$/Ru, small yet finite, and goes to zero at T_N. This is consistent with a ferromagnetic com-
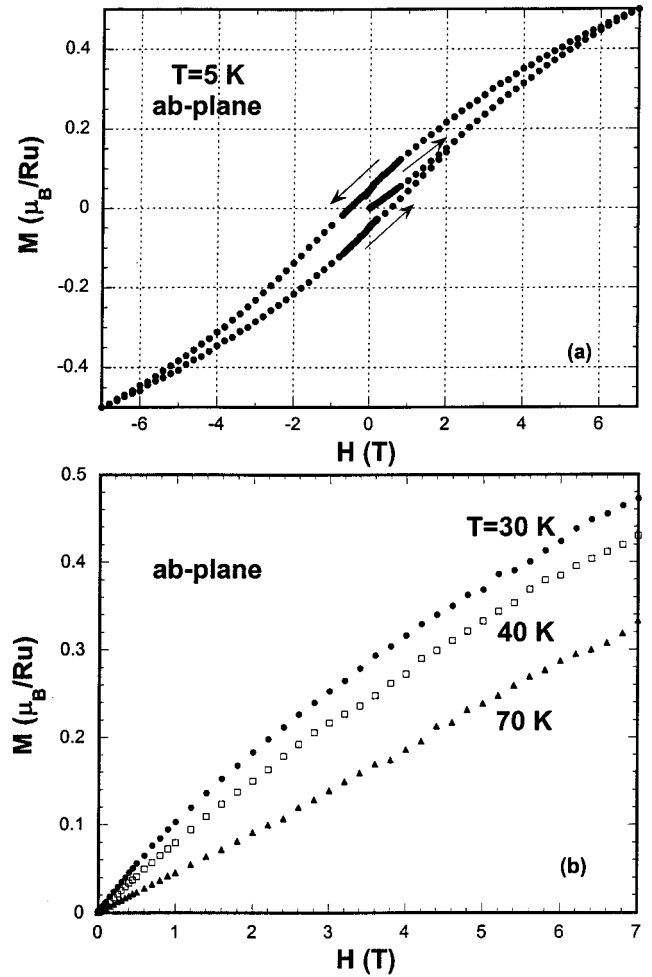
FIG. 5. Isothermal magnetization $M_{\|ab}$ at $T=5$ K (a); $M_{\|ab}$ at $T=30$, 40, and 70 K (b).

ponent due to canting of spins. (2) While the strong field dependence of M is anticipated for an antiferromagnet, the slight curvature seen in M, which confirms the presence of the ferromagnetic component, persists up to 40 K [see Fig. 5(b)]. (3) M shows no significant anisotropy when measured at different principal crystallographic directions [not shown, but it is clarified in Fig. 4(a)], which is not unexpected for a perovskitelike system such as Sr_2YRuO_6. (4) M at $H=7$ T is $0.5\mu_B$/Ru, only one-sixth of the expected ordered moment for $S=3/2$. The deficiency of the magnetic moment is a reflection of spin canting or strong spin-phonon coupling due to the severe tilting of Ru-O octahedra present in this system, which very often weakens the magnetic moment. (5) No spin flop is observed in the magnetic field range measured, indicating a lack of an easy-axis anisotropy in this system. (6) As the temperature increases, M at $H=7$ T does not change greatly until $T=70$ K [see Fig. 5(b)], suggesting the presence of strong spin fluctuations that are persistent well above T_N. As can be seen below, the spin fluctuations as well as spin-charge coupling are indeed pronounced and clearly manifested in the electrical resistivity.

Shown in Fig. 6 is the electrical resistivity $\rho(T)$ as a function of temperature for the basal plane ($1.5<T<800$ K) and for the c axis ($1.5<T<300$ K). Here $\rho(T)$
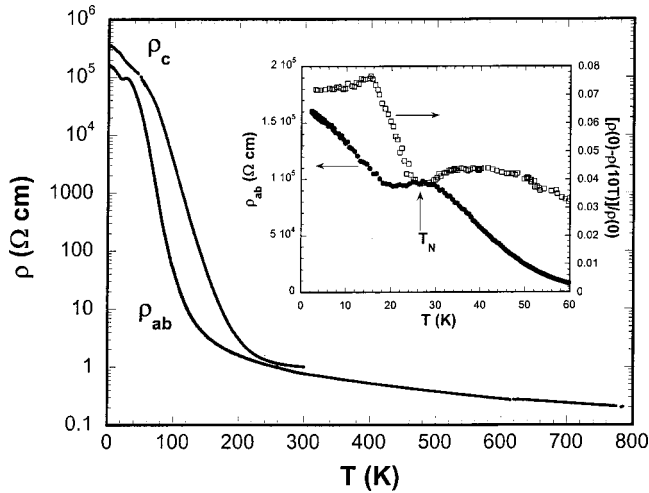
FIG. 6. Electrical resistivity ρ as a function of temperature. Inset: detailed $\rho_{ab}(T)$ below $T=60$ K (left axis), magnetoresistivity (defined as $[\rho(0\,\text{T})-\rho(10\,\text{T})/\rho(0\,\text{T})]$) as a function of temperature for $H=10$ T (right axis).

displays semiconducting or insulating behavior throughout the temperature range measured. The anisotropy between the basal plane and the c axis becomes more evident below 200 K. Here $\rho_{ab}(T)$ for the basal plane increases slowly as T decreases from 800 to 160 K and then rises rapidly below 150 K by five orders of magnitude (from 3 to 1.5 $\times 0^5$ Ω cm between 150 and 1.6 K). $\rho_{ab}(T)$ could not be fit successfully to any power law or exponential over the entire temperature range $40<T<800$ K. However, $\rho_{ab}(T)$ can be fit to $1/T$ dependence for the high-temperature range $285<T<800$ K and fits well to an activation gap of 76 meV for the intermediate-temperature range $80<T<150$ K. This value, small for an insulator, suggests a narrow charge gap and agrees well with the theoretical value (80 meV) determined from band structure calculations.[18] ρ_c obeys the activation law reasonably well for $115T<T<200$ K, yielding a gap of 120 meV. While the fitting temperature range may not be wide enough to reveal accurate activation energy, the difference in the gap could be reflective of an anisotropic electronic structure.

As T approaches T_N, $\rho(T)$ exhibits a well-defined anomaly, representing a pronounced change in spin scattering. This anomaly is much more pronounced in ρ_{ab} for the basal plane (see the inset). In the vicinity of T_N, $\rho_{ab}(T)$ clearly shows a slope change and becomes nearly temperature independent for $17<T<30$ K. Short-range magnetic order or spin fluctuations for $T\geq T_N=26$ K evident in the magnetic properties can account for the slope change in $\rho(T)$ above $T_N=26$ K: the slight decrease in $\rho_{ab}(T)$ just below T_N could be a result of a reduction of spin scattering as the system undergoes the magnetic phase transition in the vicinity of $T_N=26$ K. It is striking in that this behavior is unexpected for an ordinary antiferromagnet where the unit-cell doubling would certainly widen the insulating gap, resulting in an increase rather than a decrease in ρ. A more metallic phase in an antiferromagnetic state is conceivable in theory,[25] but rare in reality due to the sensitivity of this phase

to the degree of magnetic frustration which involves the nearest and the next-nearest neighbors.[25] It has been observed only in a handful of materials such as the stoichiometric $Ca_3Ru_2O_7$ at ambient pressure[2,9] and nonstoichiometric V_2O_3 at nonambient pressure.[26] As the temperature further decreases, a sharp transition in $\rho_{ab}(T)$ is seen at $T_M=17$ K resulting in an increase in $\rho_{ab}(T)$ by nearly 40% from T_M to 2 K. The jump in $\rho(T)$ is anomalously large, marking an evident change in the electron scattering process. The temperature dependence of $\rho_{ab}(T)$ for $2<T<7$ K very well follows the Efros-Shklovskii variable-range hopping (VRH) model with the Coulomb interaction [$\rho(T) \sim \exp(T_0/T)^{1/2}$ where T_0 is a constant associated with the localization length]. Though the fitting range may not be wide enough for an unambiguous argument, the VRH behavior with $T^{1/2}$ dependence suggests the importance of long-range Coulomb repulsions between carriers or electron correlation, which may consequently dominate the low-temperature transition region. In addition, negative magnetoresistivity, defined as $[\rho(0)-\rho(H)]/\rho(0)$, is observed and is sizable when measured at $H=10$ T (see the inset of the Fig. 6, right axis). The negative magnetoresistivity, which is already visible above $T_N(3\%-4\%)$, becomes larger below T_N, with a drop in resistivity by about 8%, and peaks just below T_M. It is clear that there is remarkably strong spin-charge coupling below T_N.

All results presented here reveal the strong interplay of spin, lattice, and charge degrees of freedom that characterizes this relatively unknown system. The magnetic ground state in Sr_2YRuO_6 is clearly unstable due to the strong competition between ferromagnetic and antiferromagnetic coupling. Theoretical calculations using the extended Stoner model conclude that in Sr_2YRuO_6 the energy difference between ferromagnetic and antiferromagnetic ordering is small compared to the magnetic stabilization energy because of the comparable Stoner factor for both ferromagnetic and antiferromagnetic structures.[18] This is due largely to the severe tilting of RuO_6 octahedra that leads to reduction of the effective hopping between neighboring Ru ions, thus weakening the effective exchange constant and, ultimately, the antiferromagnetic stabilization energy. In fact, the layered ruthenates by and large are particularly sensitive to the magnon-phonon coupling,[27] and to a large extent, it is the degree of the RuO_6 tilting that determines the ground state. This is well illustrated in all isostructural $Sr_{n+1}Ru_nO_{3n+1}$ and $Ca_{n+1}Ru_nO_{3n+1}$ ($n=1,2,3$ and infinite) where the Sr compounds tend to be ferromagnetic, whereas Ca compounds, being more distorted, lean towards antiferromagnetic coupling.[1-14] In addition, there is apparently strong spin-charge coupling, which is somewhat surprising given the overwhelmingly large resistivity and weak magnetic moment. The large resistivity can be attributed to the loose Ru-O-O-Ru linkage and the tilting of RuO_6 octahedra that reduce the overlap of orbitals, whereas the transition at T_M is likely to be associated with the Mott transition driven by correlated electrons.

[1] For review, G. Cao, C. S. Alexander, S. McCall, J. E. Crow, and R. P. Guertin, Mater. Sci. Eng., B **63**, 76 (1999).

[2] G. Cao, S. McCall, J. E. Crow, and R. P. Guertin, Phys. Rev. Lett. **78**, 1751 (1997).

[3] G. Cao, S. McCall, V. Dobrosavljevic, C. S. Alexander, J. E. Crow, and R. P. Guertin, Phys. Rev. B **61**, R5053 (2000).

[4] A. V. Puchkov, M. C. Schabel, D. N. Basov, T. Startseva, G. Cao, T. Timusk, and Z.-X. Shen, Phys. Rev. Lett. **81**, 2747 (1998).

[5] H. L. Liu, S. Yoon, S. L. Cooper, G. Cao, and J. E. Crow, Phys. Rev. B **60**, R6980 (1999).

[6] G. Cao, S. McCall, M. Shepard, J. E. Crow, and R. P. Guertin, Phys. Rev. B **56**, R2916 (1997).

[7] C. S. Alexander, G. Cao, V. Dobrosavljevic, E. Lochner, S. McCall, J. E. Crow, and R. P. Guertin, Phys. Rev. B **60**, R8422 (1999).

[8] Y. Maeno, H. Hashingmoto, K. Yoshida, S. Ishizaki, T. Fujita, J. G. Bednorz, and F. Lichtenberg, Nature (London) **372**, 532 (1994).

[9] G. Cao, K. Aboud, S. McCall, J. E. Crow, and R. P. Guertin, Phys. Rev. B **62**, 998 (2000).

[10] G. Cao, S. McCall, J. E. Crow, and R. P. Guertin, Phys. Rev. B **56**, 5387 (1997).

[11] Y. Maeno, S. Nakatsuji, and S. Ikeda, Mater. Sci. Eng., B **63**, 70 (1999).

[12] G. Cao, S. McCall, M. Shepard, J. E. Crow, and R. P. Guertin, Phys. Rev. B **56**, 321 (1997).

[13] M. Shepard, G. Cao, S. McCall, F. Freibert, and J. E. Crow, J. Appl. Phys. **79**, 4821 (1996).

[14] G. Cao, S. McCall, J. Bolivar, M. Shepard, F. Freibert, P. Henning, and J. E. Crow, Phys. Rev. B **54**, 15 144 (1996).

[15] P. C. Donohue and E. L. McCann, Mater. Res. Bull. **12**, 519 (1977).

[16] R. Greatrex, N. N. Greenwood, M. Lal, and I. Fernandez, J. Solid State Chem. **30**, 137 (1979).

[17] P. D. Battle and W. J. Macklin, J. Solid State Chem. **52**, 138 (1984).

[18] I. I. Mazin and D. J. Singh, Phys. Rev. B **56**, 2556 (1997).

[19] M. K. Wu, D. Y. Chen, D. C. Ling, and F. Z. Chien, Physica B **284**, 477 (2000).

[20] A. Knigavko and B. Rosenstein, Phys. Rev. B **58**, 9354 (1998).

[21] A. Knigavko, B. Rosenstein, and Y. F. Chen, Phys. Rev. B **60**, 550 (1999).

[22] R. M. Bozorth, Phys. Rev. Lett. **1**, 362 (1958).

[23] I. Dzyaloshinsky, J. Phys. Chem. Solids **4**, 241 (1957).

[24] T. Moriya, Phys. Rev. **120**, 91 (1960).

[25] G. Kotliar and G. Moeller, in *Spectroscopy of Mott Insulators and Correlated Metals*, edited by A. Fujimori and Y. Tokura (Springer, Berlin, 1995), pp. 15–27.

[26] For example, S. A. Carter, T. F. Rosenbaum, P. Metcal, J. M. Honig, and J. Spalek, Phys. Rev. B **48**, 16 841 (1993).

[27] D. Kirillov, Y. Suzuki, L. Antogmazza, K. Char, I. Bozovic, and T. H. Geballe, Phys. Rev. B **51**, 12 825 (1995).